

2003

# The Formin-Homology-Domain-Containing Protein FHOD1 Enhances Cell Migration

Sreenivas Koka

*Department of Oral Biology, College of Dentistry, University of Nebraska Medical Center, Lincoln, NE 68583, USA*

Cheryl L. Neudauer

*University of Minnesota Cancer Center, Minneapolis, MN 55455, USA*

Xiaodong Li

*University of Minnesota Cancer Center, Minneapolis, MN 55455, USA*

Robert E. Lewis

*Eppley Institute for Research in Cancer and Allied Diseases, Department of Biochemistry and Molecular Biology, and Department of Pathology and Microbiology, University of Nebraska Medical Center, Omaha, NE 68198, USA*

James B. McCarthy

*University of Minnesota Cancer Center, Minneapolis, MN 55455, USA*

*See next page for additional authors*

Follow this and additional works at: <http://digitalcommons.unl.edu/dentistryfacpub>

 Part of the [Other Medicine and Health Sciences Commons](#)

---

Koka, Sreenivas; Neudauer, Cheryl L.; Li, Xiaodong; Lewis, Robert E.; McCarthy, James B.; and Westendorf, Jennifer J., "The Formin-Homology-Domain-Containing Protein FHOD1 Enhances Cell Migration" (2003). *Faculty Publications, College of Dentistry*. 7.  
<http://digitalcommons.unl.edu/dentistryfacpub/7>

This Article is brought to you for free and open access by the Dentistry, College of at DigitalCommons@University of Nebraska - Lincoln. It has been accepted for inclusion in Faculty Publications, College of Dentistry by an authorized administrator of DigitalCommons@University of Nebraska - Lincoln.

---

**Authors**

Sreenivas Koka, Cheryl L. Neudauer, Xiaodong Li, Robert E. Lewis, James B. McCarthy, and Jennifer J. Westendorf

# The formin-homology-domain-containing protein FHOD1 enhances cell migration

Sreenivas Koka<sup>1</sup>, Cheryl L. Neudauer<sup>2,3</sup>, Xiaodong Li<sup>2,4</sup>, Robert E. Lewis<sup>5</sup>, James B. McCarthy<sup>2,3</sup> and Jennifer J. Westendorf<sup>2,4,\*</sup>

<sup>1</sup>Department of Oral Biology, College of Dentistry, University of Nebraska Medical Center, Lincoln, NE 68583, USA

<sup>2</sup>University of Minnesota Cancer Center, Minneapolis, MN 55455, USA

<sup>3</sup>Department of Laboratory Medicine and Pathology, Minneapolis, MN 55455, USA

<sup>4</sup>Department of Orthopaedic Surgery, Minneapolis, MN 55455, USA

<sup>5</sup>Eppley Institute for Research in Cancer and Allied Diseases, Department of Biochemistry and Molecular Biology, and Department of Pathology and Microbiology, University of Nebraska Medical Center, Omaha, NE 68198, USA

\*Author for correspondence (e-mail: weste047@umn.edu)

Accepted 23 January 2003

Journal of Cell Science 116, 1745-1755 © 2003 The Company of Biologists Ltd

doi:10.1242/jcs.00386

## Summary

Formin-homology-domain-containing proteins interact with Rho-family GTPases and regulate actin cytoskeleton organization and gene transcription. FHOD1 is a member of this family, interacts with Rac1 and induces transcription from the serum response element. In this study, we examined the effects of FHOD1 expression on cytoskeletal organization and function in mammalian cells. FHOD1 proteins were stably expressed in WM35 melanoma cells and NIH-3T3 fibroblasts. Cells expressing full-length FHOD1 demonstrated an elongated phenotype compared with vector-transfected cells and cells expressing a truncated FHOD1 (1-421) that lacks the conserved FH1 and FH2 domains. Full-length FHOD1 co-localized with filamentous actin at cell peripheries. Cells transiently expressing a C-terminal FHOD1 truncation mutant ( $\Delta$ C, residues 1-1010), which lacks an autoinhibitory protein-protein interaction domain, displayed prominent stress fibers. FHOD1 (1-421) did not induce stress fibers but localized to membrane ruffles in a manner similar to the

full-length protein, indicating that the FH1 and FH2 domains are required for stress fiber appearance. FHOD1  $\Delta$ C (1-1010)-dependent stress fibers were sensitive to dominant-negative RacN17 and the RhoA and ROCK inhibitors, C3 transferase and Y-27632. Stable overexpression of full-length FHOD1 enhanced the migration of WM35 and NIH-3T3 cells to type-I collagen and fibronectin, respectively. Cells expressing FHOD1 (1-421) migrated similar to control cells. Integrin expression and activation were not affected by FHOD1 expression. Moreover, FHOD1 overexpression did not alter integrin usage during adhesion or migration. These data demonstrate that FHOD1 interacts with and regulates the structure of the cytoskeleton and stimulates cell migration in an integrin-independent manner.

Key words: Formin homology, FHOD1, Actin cytoskeleton, Stress fibers, Migration, Cell motility, FHOS

## Introduction

Cell migration is crucial for many biological events, including embryonic development, tissue morphogenesis, inflammation, wound healing and tumor metastasis (Gumbiner, 1996; Hanahan and Weinberg, 2000; Madri and Graesser, 2000; Martin, 1997). Migration is a complex process requiring dynamic cytoskeletal reorganization and regulated interplay between cell attachment and detachment. The process consists of four phases: adhesion, spreading, contraction and tail retraction. Adhesion is dependent on matrix density, integrin density and integrin activation. Spreading requires focal complex formation, actin polymerization, Cdc42-dependent filopodia formation and Rac1-dependent lamellipodia formation (Ridley et al., 1992). Contraction occurs when traction forces are transmitted through integrin and actin-myosin cytoskeleton interactions, and involves Rho-dependent stress fiber and focal contact (or focal adhesion) formation (Ridley and Hall, 1992). Finally, tail retraction requires integrin release from the extracellular matrix and cytoskeleton, and might be the rate-limiting step in cell migration (Palecek et al., 1996).

A significant advance in our understanding of cytoskeletal dynamics is the realization that members of the formin (Fmn)/diaphanous (Dia) family of proteins [here collectively referred to as formin-homology (FH) proteins] have crucial roles in actin cytoskeleton reorganization. FH proteins are evolutionarily conserved and regulate cytokinesis and cell polarity in *Drosophila melanogaster*, *Saccharomyces cerevisiae*, *Schizosaccharomyces pombe* and *Aspergillus nidulans* (Afshar et al., 2000; Castrillon and Wasserman, 1994; Chang et al., 1997; Harris et al., 1997; Kohno et al., 1996). They also regulate conjugation in *S. pombe* (Petersen et al., 1995) and axial and bud site selection in *S. cerevisiae* (Evangelista et al., 1997; Imamura et al., 1997; Zahner et al., 1996). Recently, it was demonstrated that FH proteins in *S. cerevisiae* induce actin cable formation in an Arp2/3-independent manner prior to tropomyosin stabilization (Evangelista et al., 2002; Sagot et al., 2002) and are nucleators of unbranched and polarized actin filaments (Pruyne et al., 2002).

In mammalian cells, FH proteins regulate cytoskeletal

organization, embryonic patterning, cell survival, migration and gene transcription (Habas et al., 2001; Ishizaki et al., 2001; Jackson-Grusby et al., 1992; Sotiropoulos et al., 1999; Tominaga et al., 2000; Trumpp et al., 1992; Watanabe et al., 1997; Watanabe et al., 1999; Westendorf, 2001; Yayoshi-Yamamoto et al., 2000). *Fmn* mutations cause limb deformities and renal failure in mice (Maas et al., 1990; Woychik et al., 1985; Woychik et al., 1990; Wynshaw-Boris et al., 1997). In humans, *Dia* mutations are linked with autosomal dominant deafness (*Dia1*) and premature ovarian failure (*Dia2*) (Bione et al., 1998; Lynch et al., 1997). Increased *Dia2* expression is also directly associated with the metastatic potential of rat osteosarcoma cells (Fukuda et al., 1999). Thus, deregulated FH protein activity in mammalian cells causes developmental defects and might contribute to cancer progression.

FH proteins regulate these diverse processes by interacting with actin binding proteins and bridging Rho-family GTPases to Src tyrosine kinase and Wnt signaling pathways (Evangelista et al., 1997; Habas et al., 2001; Ishizaki et al., 2001; Kohno et al., 1996; Tominaga et al., 2000; Watanabe et al., 1997; Watanabe et al., 1999; Yayoshi-Yamamoto et al., 2000). Increasing evidence suggests that FH proteins play a crucial role in cell motility processes. A truncated, active form of the RhoA effector mDia1 is sufficient to restore force-induced focal contact formation in cells containing inactive RhoA, thereby suggesting that mDia1 is crucial for cell contraction (Riveline et al., 2001). Expression of a truncated version of mDia1 containing the Rho-binding domain inhibits the directed migration of CHO cells in a wound closure assay (Krebs et al., 2001). Similarly, expression of a truncated form of formin-related gene in leukocytes (FRL) containing the Rac1-binding domain inhibits cell spreading and chemokine-induced migration of an FRL-expressing macrophage cell line by blocking cell adhesion to fibronectin (Yayoshi-Yamamoto et al., 2000). Thus, FH proteins appear to regulate several stages of cell migration.

FHOD1 (formin-homology-2-domain-containing protein) is an FH protein that was previously described as FHOS (Westendorf, 2001; Westendorf et al., 1999). Its designation was changed to meet the Guidelines for Human Gene Nomenclature. FHOD1 is a characteristic FH family member in that it contains a GTPase binding domain (GBD), FH1 and FH2 domains, a coiled coil, and a Diaphanous-like autoregulatory domain (DAD) (Alberts, 2000; Wasserman, 1998). FHOD1 interacts with Rac1 in a guanine-nucleotide-independent manner (Westendorf, 2001). Self-interactions between the N- and C-termini prevent full-length FHOD1 from activating gene transcription from the serum response element (SRE). However, deletion of the N- or C-termini allows FHOD1 to induce SRE transcription (Westendorf, 2001). The induction of the SRE by the C-terminal FHOD1 mutant, FHOD1  $\Delta$ C, was independent of Rac1 (Westendorf, 2001). The goals of this study were to determine the effects of FHOD1 and FHOD1 C-terminal truncation mutations on cell behavior and actin cytoskeleton organization. FHOD1 and FHOD1  $\Delta$ C co-localized with F-actin at the cell periphery and in newly formed stress fibers, respectively. FHOD1 expression also induced cell elongation and enhanced the migration of WM35 melanoma cells and NIH-3T3 fibroblasts to extracellular matrix components without affecting integrin usage. These data show that expression of a full-length FH protein affects cell motility

and suggest that FH proteins are crucial regulators of cell migration.

## Materials and Methods

### FHOD1 plasmids, retroviruses and antibodies

pCMV5-HA-FHOD1 expression plasmids have been described previously (Westendorf, 2001). pMSCV-HA-FHOD1 plasmids were generated by subcloning hemagglutinin (HA) epitope-tagged FHOD1 cDNAs from pCMV5 plasmids into pMSCV via the Gateway cloning system (Invitrogen, Carlsbad, CA). This vector drives expression of FHOD1 from the murine stem cell virus (MSCV) long terminal repeat. Downstream of the FHOD1 cDNA, an internal ribosomal entry site drives the expression of enhanced green fluorescent protein (eGFP). FHOD1 retroviruses were generated by co-transfecting 293T cells with 20  $\mu$ g pMSCV and 20  $\mu$ g pCl2 (Naviaux et al., 1996; Norris et al., 1998) plasmids by calcium phosphate precipitation. Supernatants were harvested at 24 hours and 48 hours, and filtered through a 0.45  $\mu$ m syringe filter. Aliquots of the viral supernatants were stored at  $-80^{\circ}$ C.

FHOD1-N rabbit antiserum was generated by Rockland Laboratories (Gilbertsville, PA) using glutathione-S-transferase (GST)-FHOD1 (1-328) fusion protein as an immunogen. FHOD1-C mouse antiserum have been described previously (Westendorf et al., 1999).

### Generation of stable cells lines

WM35 and NIH-3T3 cells were transduced twice within 24 hours with retroviral supernatants in the presence of 8  $\mu$ g ml $^{-1}$  polybrene. eGFP expression was monitored by immunofluorescence microscopy. 2-3 days after the last transduction, eGFP-positive cells were selected by fluorescence-activated cell sorting on a FACSVantage flow cytometer (Becton Dickinson, Mountain View, CA). WM35 cells were maintained in DMEM supplemented with 10% fetal bovine serum (Biowhittaker, East Rutherford, NJ), 2 mM L-glutamine, 50 U ml $^{-1}$  penicillin and 50  $\mu$ g ml $^{-1}$  streptomycin. NIH-3T3 cells were maintained in DMEM supplemented with 10% bovine calf serum (Biowhittaker), 2 mM L-glutamine, 50 U ml $^{-1}$  penicillin and 50  $\mu$ g ml $^{-1}$  streptomycin. FHOD1 and eGFP levels were regularly monitored with immunoblotting and microscopy, respectively. Robert Kerbel (University of Toronto, Canada) generously provided the WM35 melanoma cells.

### Cell measurements

Digital phase contrast images were imported into NIH-Image, where cell lengths and widths were measured in arbitrary units. Length-to-width ratios were calculated for each cell. Isolated cells (20-34) in a minimum of three fields were measured for each cell line. Statistical significance was determined with a one-way analysis of variance.

### In situ immunofluorescence analysis

NIH-3T3 cells were grown on coverslips and transfected with expression vectors encoding HA-tagged wild-type or truncated FHOD1 proteins. Cells were washed with phosphate buffered saline (PBS) 24 hours after transfection and fixed with 4% paraformaldehyde for 5 minutes at room temperature. Cells were washed three times with PBS prior to blocking and permeabilization with 0.2% Triton X-100 in 5% normal goat serum in PBS for 30 minutes. For assays of F-actin and FHOD1 co-localization, coverslips were sequentially incubated for 30 minutes with phalloidin-rhodamine (1 U per coverslip; Molecular Probes, Eugene, OR) followed by a 1 hour incubation with rabbit anti-HA antibody (1:400, Santa Cruz Biotechnology, Santa Cruz, CA) and 1 hour incubation with fluorescein isothiocyanate (FITC)-conjugated goat anti-rabbit antibody (1:400; Jackson ImmunoResearch Laboratories, West Grove, PA).

For RacN17 experiments, NIH-3T3 cells were transiently transfected with pCMV5-FHOD1  $\Delta$ C and pCMV-T7-Rac N17. 24 hours after transfection, cells were washed in PBS and fixed with 4% paraformaldehyde (pH 7.1) in PBS for 5 minutes at room temperature prior to washing and blocking in 5% normal goat serum in PBS. For Rho pathway inhibition experiments, cells were exposed for 18 hours to C3 transferase (Rho inhibitor) or for 10 hours to Y-27632 (ROCK inhibitor). Cells were washed in cytoskeleton buffer (CB; 10 mM MES, 150 mM NaCl, 5 mM EGTA, 5 mM MgCl<sub>2</sub>, 5 mM glucose, pH 6.1) and fixed in 3% paraformaldehyde in CB for 10 minutes at room temperature. Cell were subsequently washed with CB, 0.1% Triton X-100 in CB for 1 minute prior to washing and blocking in 5% normal goat serum in PBS. For assays of F-actin and FHOD1 co-localization, coverslips were sequentially incubated for 30 minutes with phalloidin-rhodamine (1 U per coverslip; Molecular Probes) in PBS, followed by a 1 hour incubation with rabbit anti-HA antibody (1:400; Santa Cruz) and a 1 hour incubation with FITC-conjugated goat anti-rabbit antibody (1:400; Jackson ImmunoResearch Laboratories). Between and after antibody incubations, coverslips were washed in PBS and then mounted on glass slides in Vectashield mounting medium (Vector Laboratories, Burlingame, CA) and visualized at 400 $\times$  or 600 $\times$  using a Nikon confocal microscope. For assays of FHOD1  $\Delta$ C, RacN17 and F-actin co-localization, the above protocols were followed except that incubation with anti-HA antibody was followed by washing and a 1 hour incubation with mouse anti-T7 antibody (1:1000; Novagen, Madison, WI). Secondary antibodies were Cy5-labeled donkey anti-rabbit and FITC-labeled goat anti-mouse antibodies (Jackson ImmunoResearch Laboratories).

#### Immunoprecipitations

HEK293T cells were transfected with HA-tagged FHOD1 plasmids or empty vector (pCMV5) by calcium phosphate precipitation. 24 hours after transfection, the plates were placed on liquid nitrogen for 1 minute and 1 ml lysis buffer (50 mM HEPES pH 7.8, 1% Triton X-100, 1 mM EDTA, 30 mM sodium pyrophosphate, 1 mM sodium vanadate, 10 mM sodium fluoride, 1  $\mu$ M phenylmethylsulfonyl fluoride, 20 ng ml<sup>-1</sup> aprotinin) was added. Lysates were vortexed and centrifuged to pellet detergent-insoluble cell debris. Protein concentrations of lysates were determined using the BCA Protein Assay (Pierce, Rockford, IL). Equal amounts of protein were incubated for 2 hours with gentle rocking at 4°C with antibodies specific for HA (Covance, Berkeley, CA) or actin (Santa Cruz). Protein-A-Sepharose beads (Amersham Biosciences, Inc., Piscataway, NJ) were added for 20 minutes with gentle rocking at 4°C. Immune complexes were collected by centrifugation, washed twice with lysis buffer supplemented with 0.1% sodium dodecyl sulfate and then washed twice with 50 mM HEPES prior to the addition of 1 $\times$  sample buffer. Proteins from immunoprecipitations or whole cell extracts were resolved by 8-12% SDS-PAGE, electrophoretically transferred to polyvinylidene difluoride (PVDF; Schleicher & Schuell, Keene, NH) or nitrocellulose membranes (Amersham Pharmacia Biotech) and immunoblotted with primary antibodies for HA or actin, followed by the appropriate secondary antibodies. Proteins on PVDF membranes were detected using alkaline-phosphatase-conjugated secondary antibodies in a colorimetric reaction. Nitrocellulose membranes were developed with horseradish-peroxidase-conjugated secondary antibodies using the enhanced chemiluminescence system (Amersham Pharmacia Biotech).

#### Flow cytometry

Transduced WM35 cells were detached with 3 mM EDTA in PBS and washed in fluorescence buffer [1 $\times$  PBS, 2.5% bovine calf serum (BCS)]. Cells (3 $\times$ 10<sup>5</sup>) were incubated with 5  $\mu$ g ml<sup>-1</sup> of the indicated primary monoclonal antibody (mAb) for 30 minutes on ice. The cells were washed once with fluorescence buffer and then incubated for 30

minutes on ice with 5  $\mu$ g ml<sup>-1</sup> secondary antibodies conjugated to phycoerythrin or Cy5 (Jackson ImmunoResearch Laboratories). After two washes, the cells were resuspended in 1% paraformaldehyde and analyzed on FACScalibur flow cytometer. Mean fluorescence intensities of eGFP positive cells were determined using CELLQuest software (Becton Dickinson). Antibodies recognizing integrins  $\alpha_1$ ,  $\alpha_3$ ,  $\alpha_4$ ,  $\beta_4$  and  $\alpha_v\beta_3$  were purchased from Chemicon (Temecula, CA). Anti- $\alpha_2$  and 9EG7  $\beta_1$  mAbs were purchased from Pharmingen (San Diego, CA). Tucker LeBien and Yoji Shimizu (University of Minnesota, Minneapolis, MN) kindly provided the P5D2 and 15/7 $\beta_1$  Abs, respectively. Control mouse and rat antibodies were obtained from Cappel (Cochranville, PA).

#### Cell adhesion assays

Immulon 1B 96-well plates (Dynex Technologies, Chantilly, VA) were coated overnight on ice with 100  $\mu$ l of rat-tail type-I collagen (Becton Dickinson) at the indicated concentrations. Wells were blocked with PBS containing 3% (w/v) bovine serum albumin (BSA) for 1 hour at 37°C. Cells were released with 3 mM EDTA, washed twice in serum-free medium containing 20 mM HEPES, pH 7.1 (SFM/HEPES) and 1% BSA (w/v) and then resuspended to 1 $\times$ 10<sup>5</sup> cells ml<sup>-1</sup> in the same medium. For integrin-blocking assays, cells were suspended in SFM/HEPES to 1 $\times$ 10<sup>6</sup> cells ml<sup>-1</sup>, pre-incubated with 2.5  $\mu$ g ml<sup>-1</sup> of the indicated mAb for 15 minutes at 37°C and then diluted to 1 $\times$ 10<sup>5</sup> cells ml<sup>-1</sup>. Cells (1 $\times$ 10<sup>4</sup> in 100  $\mu$ l) were added to the plates and allowed to adhere to the wells for 20 minutes at 37°C. Wells were washed twice with SFM/HEPES containing 1% BSA and then twice with SFM/HEPES. Growth medium [DMEM containing 10% fetal bovine serum (FBS); 100  $\mu$ l] was added to the wells. PMS/MTS solution (CellTiter96 Aqueous Non-radioactive Cell Proliferation Assay, Promega, Madison, WI) was then added according to the manufacturer's instructions (20  $\mu$ l per well). Cells were incubated at 37°C for 3-4 hours. Absorbance at 490 nm was measured with an ELISA plate reader. The number of adherent cells was determined by normalizing to a standard curve generated with increasing volumes of the starting cell dilutions. Values represent the mean of triplicate samples.

#### Cell migration assays

Migration assays were performed in a modified Boyden chamber (NeuroProbe, Gaithersburg, MD). Cells were detached with 3 mM EDTA in PBS and washed in SFM/HEPES. Ligands [rat-tail type-I collagen, mouse type-IV collagen (Invitrogen), purified human plasma fibronectin, mouse laminin (Invitrogen) or BSA (Sigma)] were diluted in SFM/HEPES and added (33  $\mu$ l) to the lower wells. SFM/HEPES was placed in control wells. Cells (2.2 $\times$ 10<sup>4</sup> in 55  $\mu$ l) were placed in the upper wells and separated from the lower wells by polycarbonate filter with 8  $\mu$ m pores (Osmonics, Minnetonka, MN). For antibody inhibition studies, cells were pretreated with 2.5  $\mu$ g ml<sup>-1</sup> of the indicated integrin or isotype-matched control antibody (in SFM/HEPES) for 15 minutes at 37°C with rotation prior to placement in the migration chamber. Antibodies to  $\beta_1$  integrin were added at 1  $\mu$ g ml<sup>-1</sup> as this was determined to be optimal in titration experiments (data not shown). Migration assays were incubated at 37°C for 4-5 hours. Filters were fixed and stained with Diff-Quik solutions (Dade Behring, Newark, DE), and unmigrated cells were wiped from the filters. Filters were mounted on glass slides in immersion oil, and migrated cells in five random fields were counted at 400 $\times$  magnification.

## Results

### FHOD1 induces cell elongation

FHOD1 is an FH domain-containing protein that was

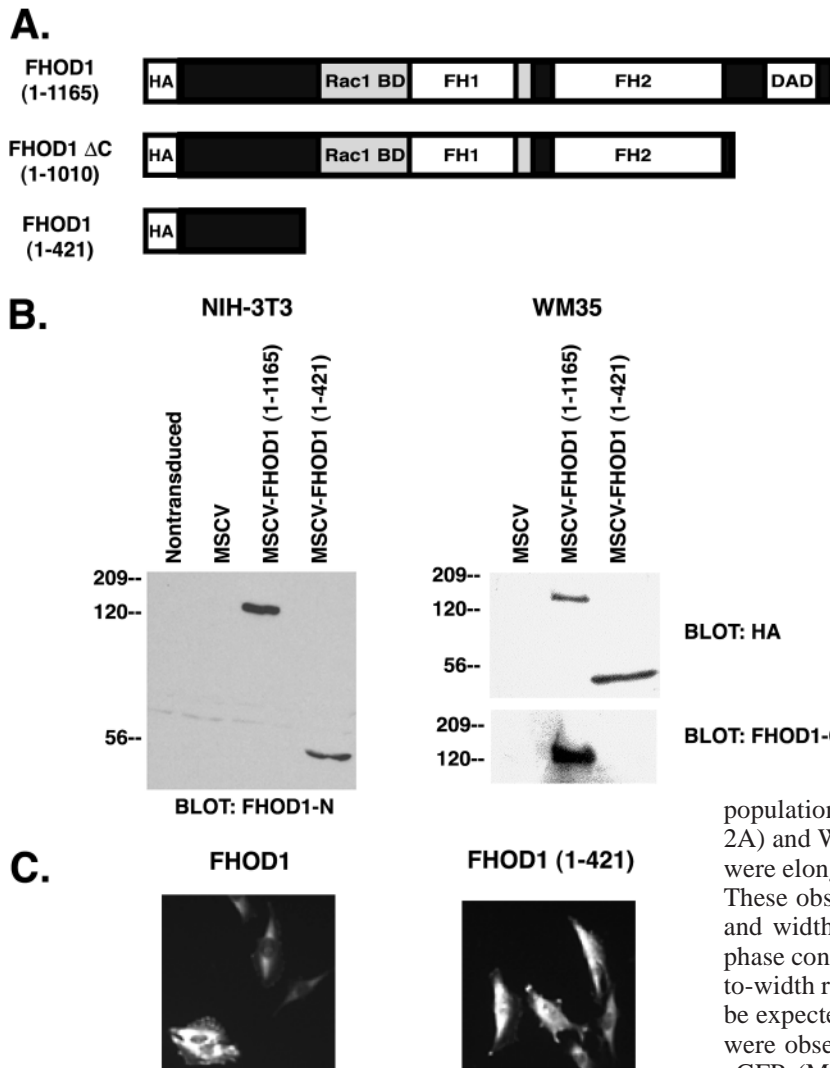


**Fig. 1.** Generation of stable FHOD1-positive WM35 and NIH-3T3 cell lines. (A) Schematic representation of the HA-FHOD1 proteins used in these studies. (B) Immunoblot analysis of endogenous and ectopic FHOD1 proteins in NIH-3T3 and WM35 cells. Protein lysates from untransduced and MSCV-transduced cells were resolved by SDS-PAGE. Antibodies recognizing the FHOD1 N-terminus (FHOD1-N) were used to probe NIH-3T3 cells for endogenous and ectopic FHOD1 proteins. WM35 cell lysates were probed with anti-HA or FHOD1-C antibodies to detect ectopic and endogenous proteins, respectively. (C) HA-FHOD1 protein subcellular localization in WM35 cells. WM35 cells were grown on coverslips and FHOD1 proteins were detected by *in situ* immunofluorescence with anti-HA antisera.

retroviruses continued to express eGFP and the FHOD1 protein for over 1 month in culture. Importantly, both full-length FHOD1 and FHOD1 (1-421) demonstrated similar localization to membrane extensions and to the perinuclear region (Fig. 1C). These results suggest that the first 421 residues play a role in targeting FHOD1 to specific subcellular locales.

An alteration in cellular morphology was observed in eGFP-positive (i.e. post-sort) populations expressing full-length FHOD1. NIH-3T3 (Fig. 2A) and WM35 (data not shown) cells that expressed FHOD1 were elongated in both confluent and subconfluent conditions. These observations were quantified by measuring the lengths and widths of subconfluent eGFP-positive NIH-3T3 cells in phase contrast images using NIH-Image software. The length-to-width ratio was calculated for each cell (Fig. 2B). As would be expected for unsynchronized cell populations, wide ranges were observed. Cells transduced with viruses expressing just eGFP (MSCV control) or truncated FHOD1 (1-421) had a mean length-to-width ratios of 13.7 and 13.1, respectively. The median value for each of these populations was 10.6. Cells expressing full-length FHOD1 displayed larger range of values with significantly different means of 20.2 ( $P < 0.05$ ). Thus, FHOD1-expressing cell populations contained elongated cells.

#### FHOD1 proteins co-localize with F-actin structures

Cell shape is regulated by the actin cytoskeleton. To determine whether FHOD1 proteins interact with and/or affect the actin cytoskeleton, NIH-3T3 cells were transiently transfected with FHOD1 expression constructs. *In situ* immunofluorescence microscopy revealed that full-length FHOD1 was expressed in perinuclear regions and at cell peripheries (Fig. 3A), which is consistent with previously reported results (Westendorf, 2001). FHOD1-expressing cells had noticeably more bundled F-actin, as detected with rhodamine-conjugated phalloidin and confocal microscopy, than adjacent nontransfected cells. FHOD1 co-localized with F-actin at the cell periphery; however, FHOD1 did not co-localize with F-actin in perinuclear regions. Moreover, dense F-actin structures away from the membrane did not appear to contain FHOD1. These data indicate that FHOD1 induces or stabilizes F-actin

previously shown to interact with the Rac1 GTPase and to stimulate transcription from the SRE (Westendorf, 2001; Westendorf et al., 1999). To gain a better understanding of its cellular function, we attempted to generate stable cell lines expressing HA-epitope-tagged full-length FHOD1 (residues 1-1165) and truncation mutants, FHOD1  $\Delta$ C (1-1010) and FHOD1 (1-421) (Fig. 1A). The human melanoma cell line WM35 and murine NIH-3T3 fibroblasts were chosen for these studies because they expressed no detectable endogenous FHOD1 (Fig. 1B). Cells were transduced with murine stem cell retroviruses that express HA-FHOD1 proteins from the MSCV long terminal repeat and eGFP from an internal ribosomal entry site. 3-5 days after transduction, cells were selected by fluorescence-activated cell sorting for eGFP expression. 5-7 days later, FHOD1 expression was analyzed by immunoblot analysis with HA- or FHOD1-specific antibodies. Full-length FHOD1 and FHOD1 (1-421) were detected in both NIH-3T3 and WM35 cells (Fig. 1B). However, FHOD1  $\Delta$ C expression was never detected in sorted eGFP positive cell lines, although it was present 2 days after transduction and prior to cell sorting (data not shown). Thus, our construct was functional but FHOD1  $\Delta$ C was not tolerated long-term in cell cultures. Cells transduced with the full-length FHOD1 or FHOD1 (1-421)

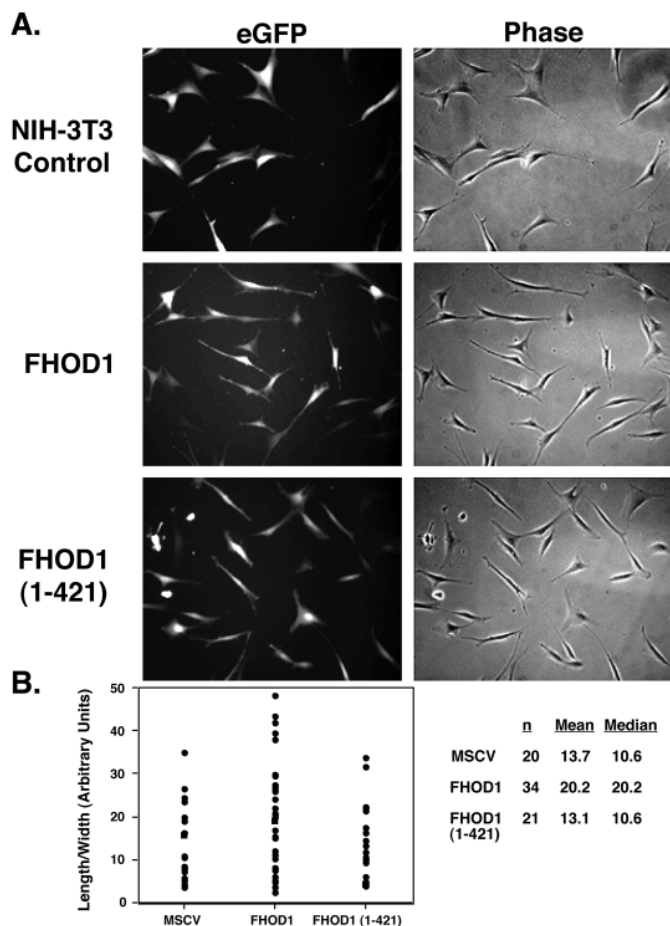


**Fig. 2.** FHOD1 induces cell elongation. (A) Fluorescent (left) and phase contrast (right) images of transduced and sorted NIH-3T3 cells showing the cell morphology of eGFP-expressing cells. Because the same vector encodes FHOD1 and eGFP, eGFP expression is used as a marker to detect FHOD1-expressing cells. (B) FHOD1-positive cell populations contain elongated cells. The length-to-width ratios of eGFP positive cells are plotted in the graph. The table indicates the mean and median values for the indicated population. \* $P < 0.05$  for FHOD1 versus MSCV and FHOD1 (1-421) cells.

formation but that interactions between FHOD1 and F-actin are only present at the cell periphery.

We previously demonstrated that N- and C-terminal domains in FHOD1 mediate an intramolecular interaction(s) (Westendorf, 2001). Deletion of the self-interaction domains creates active FHOD1 proteins that stimulate transcription via alternative signaling pathways. Differential cellular localization of the FHOD1 mutants appears to be responsible for these effects (Westendorf, 2001). To expand these studies, we examined how FHOD1 truncation mutants interact with the actin cytoskeleton. Cells expressing FHOD1  $\Delta$ C demonstrated markedly thick stress fibers. FHOD1  $\Delta$ C co-localized with the stress fibers (Fig. 3A, Fig. 4B). Cells expressing FHOD1 (1-421) did not display stress fibers but, like cells containing full-length FHOD1, appeared to have more F-actin than untransfected cells in the same field. FHOD1 (1-421) also co-localized with F-actin at the cell membrane and in the perinuclear region. These results indicate that the N-terminus of FHOD1 is sufficient for localization to the membrane and

perinucleus. These results demonstrate that an activated form of FHOD1 induces or stabilizes stress fiber formation.

To determine whether FHOD1 proteins also interact with globular (G) actin, HEK293T cells were transiently transfected with full-length or truncated HA-FHOD1 proteins and assayed by immunoprecipitation and immunoblotting analysis. Full-length FHOD1 co-immunoprecipitated with Triton X-100 soluble actin (Fig. 3B). However, the truncation mutants, FHOD1 (1-421), [1-1010 ( $\Delta$ C)] and (469-1165), did not interact with G-actin. These results suggest that FHOD1 associates with G-actin and that multiple regions of FHOD1 contribute to the interaction.

#### FHOD1- $\Delta$ C-dependent stress fibers require Rac1, RhoA and ROCK activities

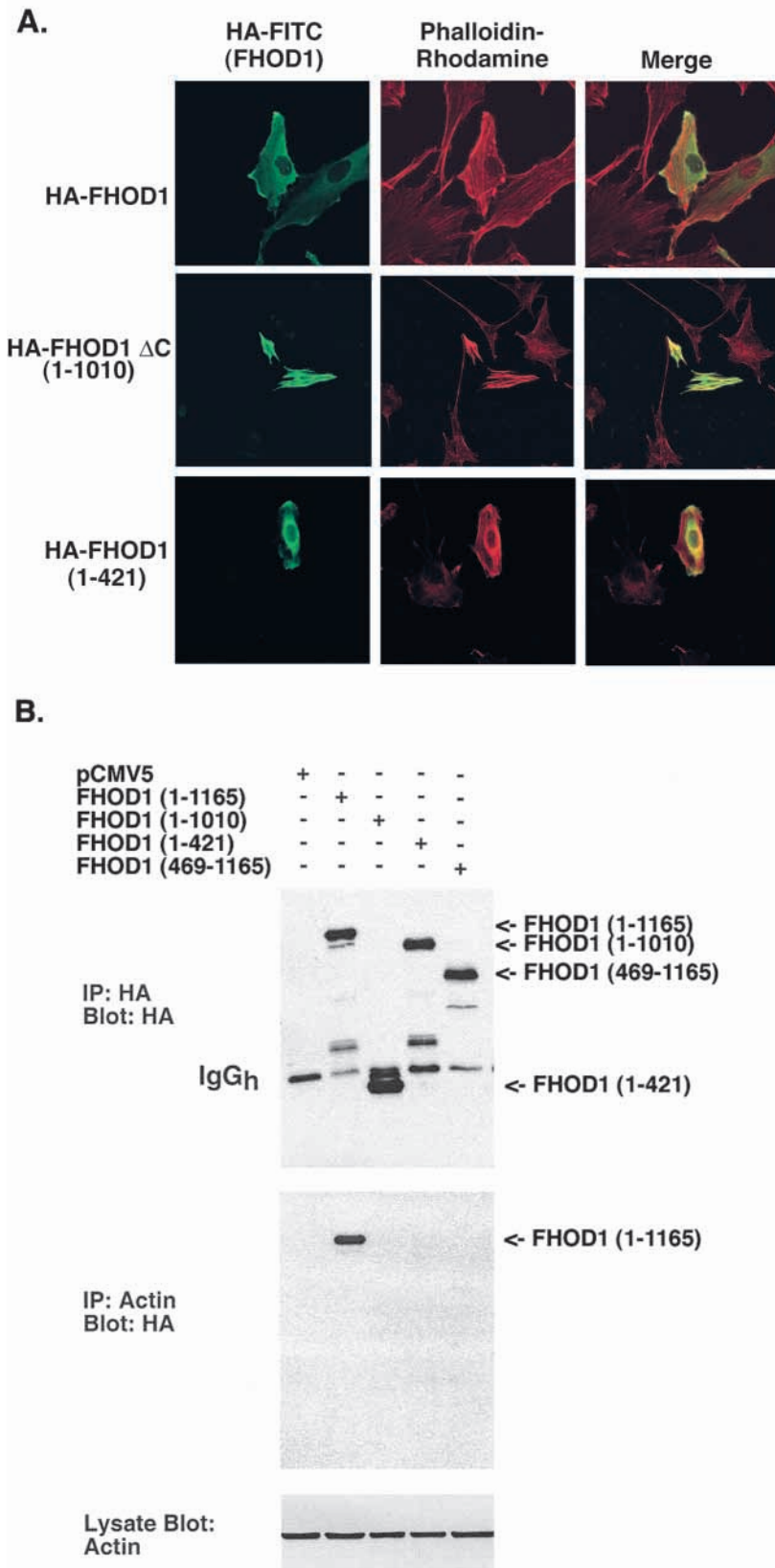
We previously demonstrated that FHOD1 interacts with Rac1 but not RhoA (Westendorf, 2001). To determine whether Rac1 is required for FHOD1- $\Delta$ C-dependent stress fiber formation, we transiently co-transfected NIH-3T3 cells with FHOD1  $\Delta$ C and dominant-negative RacN17. Actin stress fiber organization in cells expressing both FHOD1  $\Delta$ C and RacN17 was similar to neighboring, non-transfected cells that displayed normal actin-rich lamellipodia (Fig. 4A). Thus, RacN17 prevented the appearance of stress fibers in FHOD1 $\Delta$ C-expressing cells. These data suggest that FHOD1 is upstream of Rac1.

We also tested the effects of RhoA and ROCK inhibitors, C3 transferase and Y-27632, on FHOD1-dependent stress fibers. Stress fiber formation requires RhoA and its downstream effector ROCK (Amano et al., 1997; Leung et al., 1996; Ridley and Hall, 1992). C3 transferase (Rho inhibitor; Fig. 4B) and Y-27632 (ROCK inhibitor; Fig. 4C) inhibited FHOD1- $\Delta$ C-dependent stress fibers. These inhibitors induced a phenotype seen with Rho inhibition by RhoGAP (Tatsis et al., 1998; Vincent and Settleman, 1999). Together these data demonstrate that FHOD1-dependent stress fibers required Rac1, RhoA and ROCK enzymatic activities.

#### FHOD1 enhances cell migration without affecting adhesion, integrin usage or integrin activation

The altered morphology of FHOD1-expressing cells suggested that FHOD1 might affect cell adhesion and/or motility. To determine whether FHOD1 affects cell adhesion, transduced WM35 cells were allowed to adhere to various concentrations of type-I collagen. The number of adherent cells increased in a type-I collagen concentration-dependent manner and peaked at  $15 \mu\text{g ml}^{-1}$  (Fig. 5A). FHOD1-expressing cells bound to the substrate similar to control (empty pMSCV vector) and FHOD1 (1-421)-positive cells. Likewise, the adherence of FHOD1-positive and control NIH-3T3 cells to fibronectin was comparable (Fig. 5B). These data indicate that FHOD1 does not affect the overall adherence of cells to these extracellular matrix proteins.

Although cell adhesion was not affected by FHOD1 expression, motility towards extracellular matrix proteins was significantly enhanced in both WM35 and NIH-3T3. An approximate two- to threefold increase in the migration of FHOD1-positive WM35 melanoma cells to type-I collagen was observed (Fig. 6A). Migration was concentration dependent, but FHOD1-positive cells had increased migration at each



concentration relative to control (MSCV) and FHOD1 (1-421)-expressing cells. WM35 cells did not migrate to BSA or fibronectin (data not shown).

**Fig. 3.** FHOD1 interacts with F-actin and G-actin. (A) NIH-3T3 cells were transiently transfected with plasmids encoding full-length HA-FHOD1 (1-1165), HA-FHOD1 ΔC (1-1010) or HA-FHOD1 (1-421). FHOD1 expression was detected by in situ staining with anti-HA followed by FITC-conjugated secondary antibodies. Cells were counterstained with phalloidin-rhodamine to detect F-actin. Images were collected by confocal microscopy. (B) HEK293T cells were transiently transfected with expression vectors for the indicated HA-FHOD1 proteins. Triton X-100 soluble cellular proteins were immunoprecipitated with anti-HA or anti-actin antibodies. Proteins were detected by immunoblotting with anti-HA or anti-actin antibodies and enhanced chemiluminescence.

FHOD1-positive NIH-3T3 cells also displayed increased migration to extracellular matrix proteins. FHOD1-expressing cells had increased migration to fibronectin and laminin compared with control (MSCV) and FHOD1 (1-421)-expressing cells (Fig. 6B). Similar results were observed when 10% BCS, which contains fibronectin and laminin along with other stimulatory molecules, was used as a migratory signal. None of the NIH-3T3 cells migrated in response to BSA (Fig. 6B), or type-I or type-IV collagen (data not shown). Together, these data indicate that FHOD1 expression enhances cell migration in both fibroblasts and melanoma cells.

To begin to understand the mechanism of FHOD1-enhanced cell migration, we examined integrin expression levels and the adhesion properties of FHOD1-expressing and control WM35 melanoma cell lines. WM35 cells expressed  $\alpha_1$ ,  $\alpha_2$ ,  $\alpha_3$ ,  $\alpha_4$ ,  $\beta_1$  and  $\alpha v\beta_3$  at varying levels. FHOD1-positive cells had slightly elevated integrin levels as compared to control (MSCV) and FHOD1 (1-421)-expressing cells (Fig. 7A) but the mean fluorescence intensities varied by less than 10%.

To determine whether FHOD1 expression affected integrin function in adhesion and migration, we preincubated control (MSCV) and FHOD1-positive WM35 cells with anti-integrin blocking antibodies prior to placing them in adhesion and migration assays. The  $\alpha_1\beta_1$ ,  $\alpha_2\beta_1$ ,  $\alpha_3\beta_1$  and  $\alpha v\beta_3$  integrins mediate binding to type-I collagen (van der Flier and Sonnenberg, 2001). These integrin subunits were all expressed in the WM35 cells (Fig. 7A). Blocking antibodies to  $\beta_1$  integrin completely inhibited the adhesion and migration of control (MSCV) and FHOD1-positive cells (Fig. 7B,C). Blocking antibodies to  $\alpha_1$  and  $\alpha_2$  each partially blocked adhesion and migration of control (MSCV) and FHOD1-expressing WM35 cells. Antibodies blocking  $\alpha_3$  (Fig. 7B,C) and  $\alpha v\beta_3$  (data not shown) did not block the adhesion or migration of any WM35 cell populations. Thus, WM35 cell adhesion to type-I collagen is largely mediated by  $\alpha_1\beta_1$  and  $\alpha_2\beta_1$  integrin complexes. Importantly, FHOD1 expression did



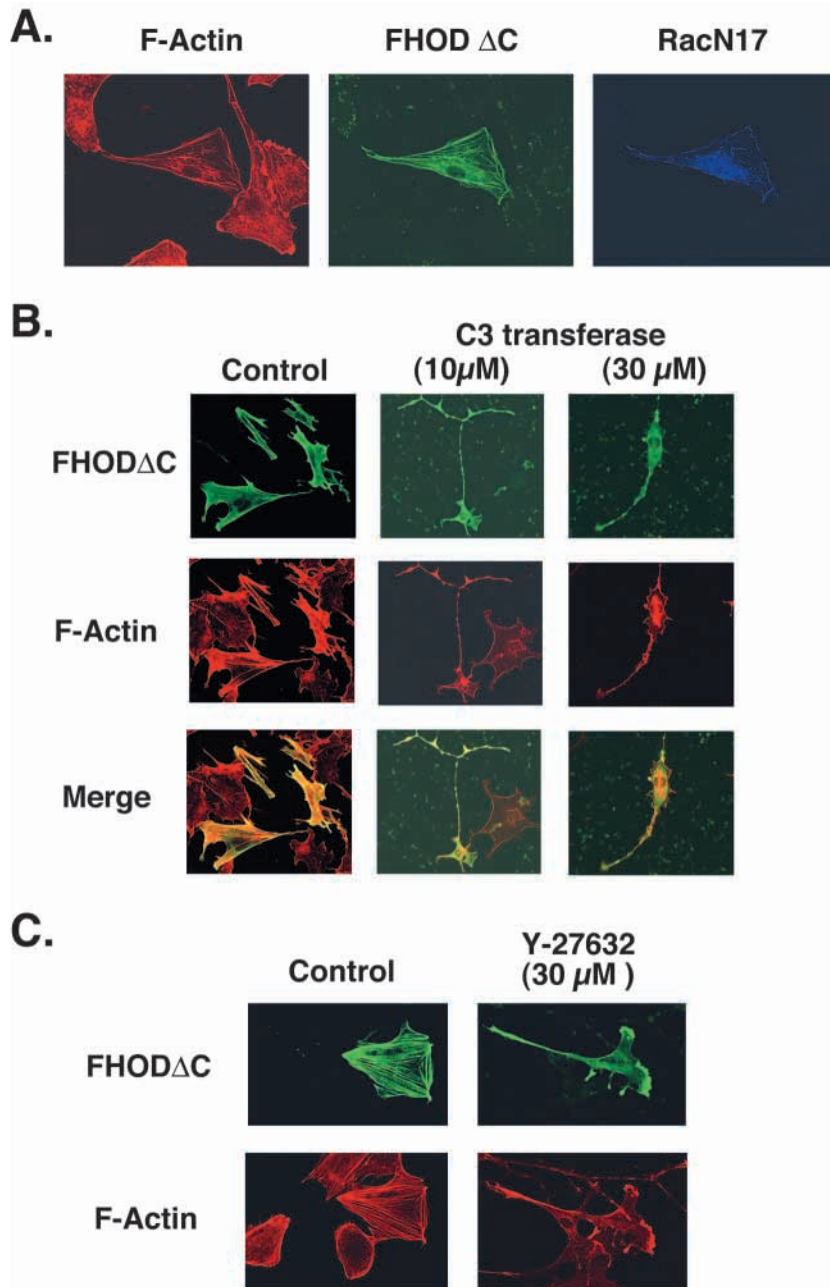


**Fig. 4.** Dominant-negative Rac1 and inhibitors of RhoA and ROCK block FHOD1  $\Delta$ C-dependent stress fibers. (A) Rac1N17 blocks FHOD1- $\Delta$ C-dependent stress fibers. NIH-3T3 cells were transiently transfected with pCMV5-FHOD1  $\Delta$ C and pCMV-T7-Rac1N17. FHOD1- and Rac1N17-expressing cells were detected by in situ immunofluorescence. F-actin was detected with phalloidin-rhodamine. (B) RhoA activity is required for FHOD1- $\Delta$ C-dependent stress fibers. FHOD1- $\Delta$ C-transfected NIH-3T3 cells were incubated for 18 hours with 10  $\mu$ M or 30  $\mu$ M C3 transferase prior to in situ fluorescence analysis and confocal microscopy. (C) ROCK activity is required for FHOD1- $\Delta$ C-dependent stress fiber formation. FHOD1- $\Delta$ C-transfected NIH-3T3 cells were incubated for 10 minutes with 30  $\mu$ M Y-27632. FHOD1  $\Delta$ C and F-actin were detected with in situ fluorescence and confocal microscopy.

aggressive tumor cells and is associated with poor prognosis. Cell motility requires local filament polymerization at the leading edge of the cell. This occurs in response to extracellular stimuli and is mediated largely by Rho-family GTPases through downstream effector molecules. FH-domain-containing proteins are one class of Rho family effectors that regulate cytoskeleton structure. In this report, we show that the Rac1-interacting FH protein FHOD1 enhanced cell motility to extracellular matrix proteins in an integrin-independent manner when expressed in fibroblasts and melanoma cells. FHOD1 co-localized with F-actin at the cell periphery. These data suggest a mechanism for enhanced cell migration in which FHOD1 plays a role in F-actin formation and/or stabilization of the leading edge.

Together with previous reports, our data indicate that FH proteins might affect multiple phases of cell migration. Truncated active forms of mDia1 that lack the N-terminal RhoA-binding domain restore force-induced focal contact formation in cells in which RhoA is inactivated, suggesting that mDia is crucial for cell contraction and acts downstream of RhoA (Riveline et al., 2001). Krebs and colleagues demonstrated that expression of a truncated version of mDia1 containing the FH3 domain and GBD inhibits the directed cell migration of CHO cells in a wound closure assay (Krebs et al., 2001). Third, a truncated form of FRL containing the FH3 and Rac1-binding domains inhibits cell spreading and chemokine-induced migration of an FRL-expressing macrophage cell line by blocking cell adhesion to fibronectin (Yayoshi-Yamamoto et al., 2000). These latter two reports suggest that the N-termini of FH proteins are sufficient to interfere with migration, possibly by inhibiting the respective endogenous FH protein. We did not observe significant inhibition of migration upon FHOD1 (1-421) expression. However, this fragment lacks the GBD and thus might not block the appropriate signaling pathways.

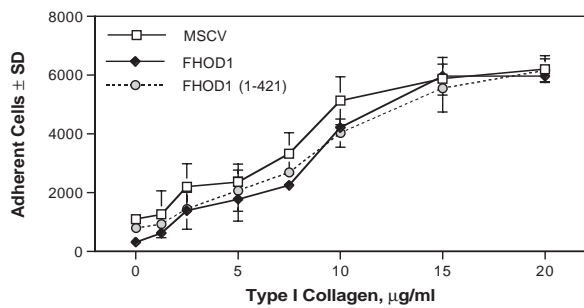
One novel aspect of our study is the long-term expression

not alter the ability of these integrins to mediate cell adhesion or migration. FHOD1 also did not affect the appearance of activation-dependent  $\beta$ 1 integrin conformation epitopes, 15/7 (Yednock et al., 1995) or 9EG7 (Lenter et al., 1993), in WM35 cells (Fig. 8). Divalent cations ( $MnCl_2$ ) increased these epitopes to similar levels in both MSCV- and FHOD1-expressing WM35 (data not shown). These data indicate that FHOD1 does not affect the avidity or affinity of integrins. Thus, FHOD1 probably enhances cell migration by activating events downstream of integrins.

## Discussion

Cell migration is required for embryonic and organ development, inflammatory responses and wound healing. Enhanced cell motility or metastasis is also a hallmark of

**A. WM35**



**B. NIH-3T3**

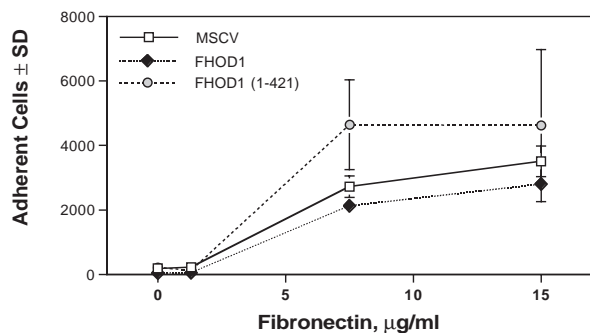
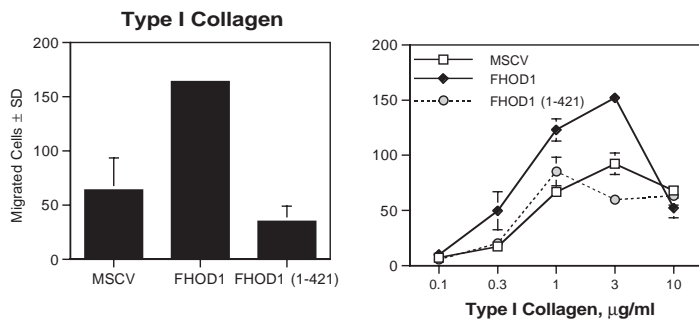
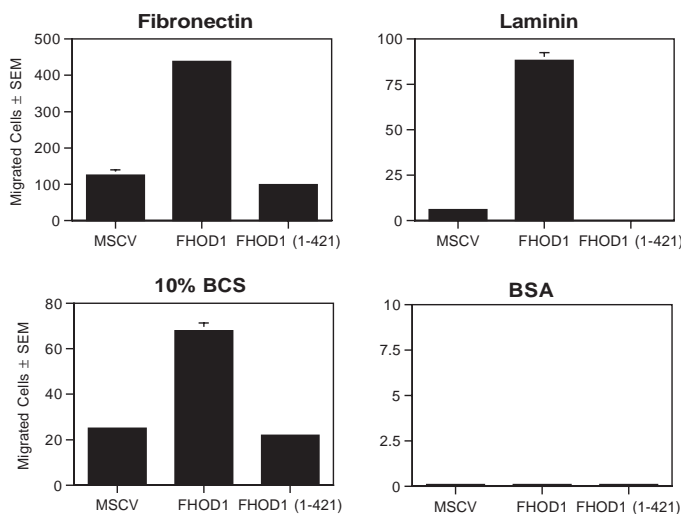


**Fig. 5.** FHOD1 expression does not affect cell adhesion. (A) FHOD1 expression does not significantly affect WM35 cell adhesion to type-I collagen. WM35 cells were allowed to adhere to plates coated with the indicated concentrations of type-I collagen for 20 minutes. Adherent cells were quantified with a cell viability assay. The number of adherent cells was normalized to a standard curve generated by plating increasing numbers of cells. (B) FHOD1 expression does not significantly affect NIH-3T3 cell adhesion to fibronectin. NIH-3T3 cells were allowed to adhere to plates coated with the increasing concentrations of fibronectin for 20 minutes. The number of adherent cells was determined as described in A.

**A. WM35**



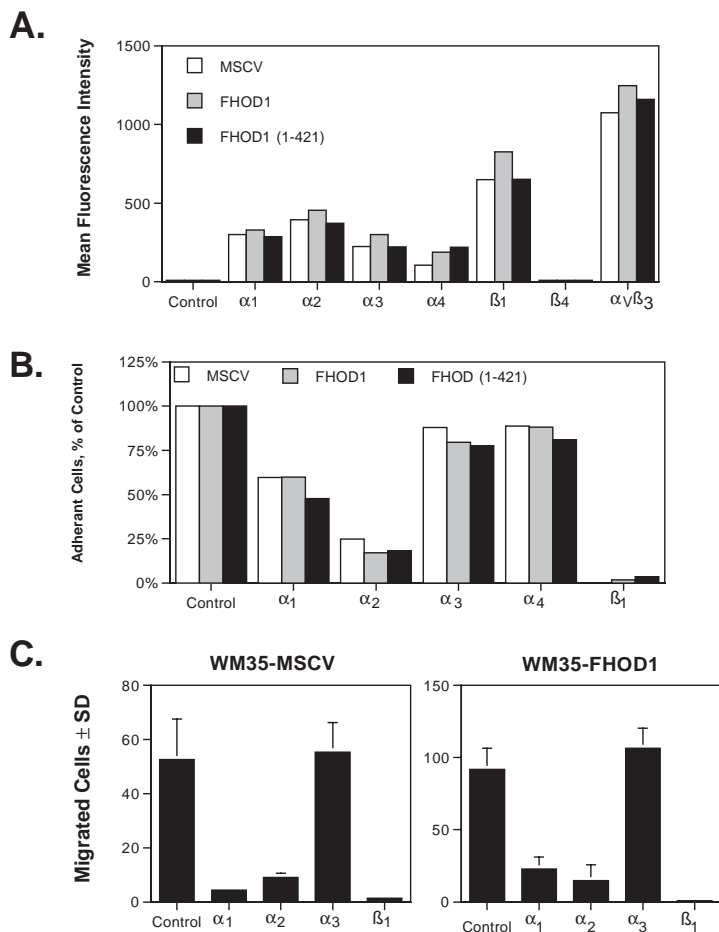
**B. NIH-3T3**



and analysis of a full-length FH protein. All previous studies examining the roles of FH proteins in cell migration were performed with fragments of the respective FH protein that have not been identified in nature. Attempts to overexpress Fmn and FRL were reportedly unsuccessful, leading the investigators to conclude that stable expression of these FH proteins is toxic (Vogt et al., 1993; Yayoshi-Yamamoto et al., 2000). We were able to obtain long-term cultures of FHOD1-overexpressing NIH-3T3 and WM35 cells. Our results might be dependent on our choice of expression systems but it is also possible that FHOD1 has a distinct role and that its overexpression does not place the cells at a selective disadvantage. Interestingly, our attempts to generate stable FHOD1  $\Delta C$  expression were unsuccessful. The predominant stress fibers found in cells transiently transfected with this truncated and activated FHOD1 protein probably prohibit long-term survival. These results suggest that individual FH proteins might perform specialized functions and link the actin cytoskeleton to different signaling pathways to control cell activities.

FHOD1 was localized to cell membranes and perinuclear regions in both stable and transient transfectants (Fig. 1C, Fig. 3A). This staining pattern is similar to that observed for mDia1 (Watanabe et al., 1997). Interestingly, FHOD1 co-localized with F-actin in lamellae but not with F-actin in the cytoplasm. These results suggest that FHOD1 participates in filamentous actin polymerization or nucleation at the cell membrane. The induction of stress fiber formation in cells expressing an activated FHOD1 protein lacking the C-terminal autoregulatory domain has also been observed by others (Oliver Fackler, personal communication) and indicates that FHOD1 might have a role in actin polymerization. These results agree well with the recent findings that FH proteins in *S. cerevisiae* control cell polarity by nucleating actin cable assembly independent of Arp2/3 proteins

**Fig. 6.** FHOD1 enhances cell migration. (A) Expression of full-length FHOD1 in WM35 cells enhanced migration to type-I collagen. The migration of control (MSCV) and FHOD1-expressing WM35 cells to type-I collagen (1  $\mu\text{g ml}^{-1}$  on the left, indicated concentrations on the right) during a 4-5 hour period was measured in a Boyden chamber. (B) Expression of full-length FHOD1 in NIH-3T3 cells enhanced migration to fibronectin, laminin and BCS. Each protein was used at a final concentration of 1  $\mu\text{g ml}^{-1}$ . BCS was added at 10% (v/v). Cells were allowed to migrate for 4-5 hours in a modified Boyden chamber.



(Evangelista et al., 2002; Pruyne et al., 2002; Sagot et al., 2002). The nature of FHOD1 interactions with F-actin remains to be determined. Full-length FHOD1 did interact with G-protein monomers in vivo, but truncated FHOD1 proteins did not. These data suggest that FHOD1 associates indirectly with actin and/or that multiple regions of FHOD1 are necessary to interact with actin or actin-binding proteins. One likely candidate is profilin, which binds to the proline-rich FH1 domain of other FH proteins (Chang et al., 1997; Evangelista et al., 1997; Umikawa et al., 1998; Watanabe et al., 1997; Yayoshi-Yamamoto et al., 2000).

Many studies indicate that FH proteins are involved in actin organization and the appearance of stress fibers. Truncated and activated versions of mDia1, a downstream effector of RhoA (Watanabe et al., 1997), induce thin actin stress fibers that are

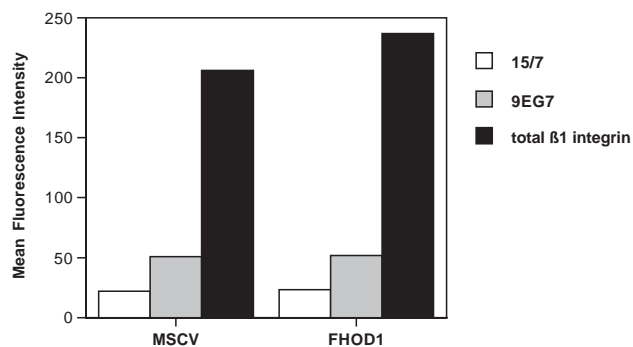


**Fig. 7.** FHOD1 expression does not affect integrin expression or use. (A) FHOD1 does not significantly alter integrin expression on WM35 cells. Stable WM35 cells were incubated with PE-conjugated anti-integrin antibodies and analyzed by flow cytometry. The mean PE fluorescence intensity of eGFP-positive cells was determined with CellQuest software. (B) FHOD1 expression does not alter integrin usage during cell adhesion. Cells were preincubated for 20 minutes with  $2.5 \mu\text{g ml}^{-1}$  of the isotype-matched control or the indicated  $\alpha$ -integrin mAb, or with  $1 \mu\text{g ml}^{-1}$  of anti- $\beta_1$  mAb. The amount of cell adhesion to plates coated with  $15 \mu\text{g ml}^{-1}$  type-I collagen within 20 minutes was determined with a cell viability assay. Values for each cell line were normalized to the control cells incubated with the isotype-matched mAb. (C) FHOD1 does not alter integrin usage during cell migration. WM35-MSCV control (left) or FHOD1-expressing (right) cells were preincubated for 20 minutes with  $2.5 \mu\text{g ml}^{-1}$  of the isotype-matched control or the indicated  $\alpha$ -integrin mAb or with  $1 \mu\text{g ml}^{-1}$  of anti- $\beta_1$  mAb. Cell migration during a 4.5 hour period was measured in a modified Boyden chamber assay.

subsequently organized into thick stress fibers by another RhoA effector, ROCK (Watanabe et al., 1999). In this report, we demonstrate that a truncated version of FHOD1 (residues 1-1010) also induces stress fibers. These actin structures were inhibited by a dominant-negative Rac1 (N17) protein. The ROCK and RhoA inhibitors Y-27632 and C3 transferase also prevented stress fiber formation. These data suggest that FHOD1 acts upstream of Rac1, RhoA and ROCK. We previously placed Rac1 downstream of FHOD1 in pathways activating transcription from the SRE (Westendorf, 2001). Thus, there might exist multiple classes of FH proteins, those that act upstream of Rho family GTPases and those that are Rho GTPase effectors. FHOD1 and Daam1, a Wnt-activated FH protein that regulates RhoA (Habas et al., 2001), are members of the former class, whereas mDia belongs in the latter. The signals that activate FHOD1 remain to be identified. However, it is clear that FH proteins have multiple, complex roles in the organization of actin structures.

In summary, we found that FHOD1 co-localized with some F-actin structures at the cell periphery. We also found that long-term FHOD1 expression induced cell elongation and enhanced migration of fibroblasts and melanomas cells. A FH gene (a *mDia2* homolog) was identified as being overexpressed differently in highly metastatic rat osteosarcoma cells (Fukuda et al., 1999). Thus, increased FH protein expression might play a role in tumor metastasis by facilitating actin polymerization. Subsequent stabilization of actin filaments would lead to the formation of contractile bundles that are important for cell motility (Feldner and Brandt, 2002). Our data indicate that FHOD1 expression increases migration without altering integrin expression, affinity or avidity. Future studies will

**Fig. 8.** FHOD1 expression does not affect  $\beta_1$ -integrin activation. MSCV and FHOD1-expressing WM35 cells were incubated with antibodies recognizing the  $\beta_1$ -integrin activation epitopes 15/7 and 9EG7, the pan- $\beta_1$ -integrin epitope P5D2 or control IgG for 30 minutes on ice followed by a 30-minute incubation with a Cy5-conjugated secondary mAb. Mean fluorescent intensities of eGFP-positive cells were determined with CellQuest software and normalized to baseline levels of control antibodies.

address the roles of FHOD1 in regulating events downstream of integrins to better understand its role in cell motility and potentially tumor metastasis.

We thank You Zhou and Christian Elowsky of the Microscopy Core Facility (University of Nebraska-Lincoln) for their helpful assistance. We also thank the staff of the Flow Cytometry Core Facility (University of Minnesota Cancer Center, a comprehensive cancer center designated by the National Cancer Institute), supported in part by P30 CA77598. The University of Minnesota Cancer Center, Minnesota Medical Foundation and National Institutes of Health (RO1 CA82295 to J.B.M.) supported this work.

## References

- Afshar, K., Stuart, B. and Wasserman, S. A.** (2000). Functional analysis of the *Drosophila* diaphanous FH protein in early embryonic development. *Development* **127**, 1887-1897.
- Alberts, A. S.** (2000). Identification of a carboxy-terminal diaphanous-related formin homology protein autoregulatory domain. *J. Biol. Chem.* **276**, 2824-2830.
- Amano, M., Chihara, K., Kimura, K., Fukata, Y., Nakamura, N., Matsuura, Y. and Kaibuchi, K.** (1997). Formation of actin stress fibers and focal adhesions enhanced by Rho-kinase. *Science* **275**, 1308-1311.
- Bione, S., Sala, C., Manzini, C., Arrigo, G., Zuffardi, O., Banfi, S., Borsani, G., Jonveaux, P., Philippe, C., Zuccotti, M. et al.** (1998). A human homologue of the *Drosophila melanogaster* diaphanous gene is disrupted in a patient with premature ovarian failure: evidence for conserved function in oogenesis and implications for human sterility. *Am. J. Hum. Genet.* **62**, 533-541.
- Castrillon, D. H. and Wasserman, S. A.** (1994). *Diaphanous* is required for cytokinesis in *Drosophila* and shares domains of similarity with the products of the *limb deformity* gene. *Development* **120**, 3367-3377.
- Chang, F., Drubin, D. and Nurse, P.** (1997). cdc12p, a protein required for cytokinesis in fission yeast, is a component of the cell division ring and interacts with profilin. *J. Cell Biol.* **137**, 169-182.
- Evangelista, M., Blundell, K., Longtine, M. S., Chow, C. J., Adames, N., Pringle, J. R., Peter, M. and Boone, C.** (1997). Bni1p, a yeast formin linking cdc42p and the actin cytoskeleton during polarized morphogenesis. *Science* **276**, 118-122.
- Evangelista, M., Pruyne, D., Amberg, D. C., Boone, C. and Bretscher, A.** (2002). Formins direct Arp2/3-independent actin filament assembly to polarize cell growth in yeast. *Nat. Cell Biol.* **4**, 32-41.
- Feldner, J. C. and Brandt, B. H.** (2002). Cancer cell motility – on the road from c-erbB-2 receptor steered signaling to actin reorganization. *Exp. Cell Res.* **272**, 93-108.
- Fukuda, T., Kido, A., Kajino, K., Tsutsumi, M., Miyauchi, Y., Tsujiuchi, T., Konishi, Y. and Hino, O.** (1999). Cloning of differentially expressed genes in highly and low metastatic rat osteosarcomas by a modified cDNA-AFLP method. *Biochem. Biophys. Res. Commun.* **261**, 35-40.
- Gumbiner, B. M.** (1996). Cell adhesion: the molecular basis of tissue architecture and morphogenesis. *Cell* **84**, 345-357.
- Habas, R., Kato, Y. and He, X.** (2001). Wnt/Frizzled activation of Rho regulates vertebrate gastrulation and requires a novel Formin homology protein Daam1. *Cell* **107**, 843-854.
- Hanahan, D. and Weinberg, R. A.** (2000). The hallmarks of cancer. *Cell* **100**, 57-70.
- Harris, S. D., Hamer, L., Sharpless, K. E. and Hamer, J. E.** (1997). The *Aspergillus nidulans* *sepA* gene encodes an FH1/2 protein involved in cytokinesis and the maintenance of cellular polarity. *EMBO J.* **16**, 3474-3483.
- Imamura, H., Tanaka, K., Hihara, T., Umikawa, M., Kamei, T., Takahashi, K., Sasaki, T. and Takai, Y.** (1997). Bni1p and Bnr1p: downstream targets of the Rho family small G-proteins which interact with profilin and regulate actin cytoskeleton in *Saccharomyces cerevisiae*. *EMBO J.* **16**, 2745-2755.
- Ishizaki, T., Morishima, Y., Okamoto, M., Furuyashiki, T., Kato, T. and Narumiya, S.** (2001). Coordination of microtubules and the actin cytoskeleton by the Rho effector mDial1. *Nat. Cell Biol.* **3**, 8-14.
- Jackson-Grusby, L., Kuo, A. and Leder, P.** (1992). A variant *limb deformity* expressed in the embryonic mouse limb defines a novel formin. *Genes Dev.* **6**, 29-37.
- Kohno, H., Tanaka, K., Mino, A., Umikawa, M., Imamura, H., Fujiwara, T., Fujita, Y., Hotta, K., Qadota, H., Watanabe, T. et al.** (1996). Bni1p implicated in cytoskeletal control is a putative target of Rho1p small GTP binding protein in *Saccharomyces cerevisiae*. *EMBO J.* **15**, 6060-6068.
- Krebs, A., Rothkegel, M., Klar, M. and Jockusch, B. M.** (2001). Characterization of functional domains of mDial1, a link between the small GTPase Rho and the actin cytoskeleton. *J. Cell Sci.* **114**, 3663-3672.
- Lenter, M., Uhlig, H., Hamann, A., Jenö, P., Imhof, B. and Vestweber, D.** (1993). A monoclonal antibody against an activation epitope on mouse integrin chain beta 1 blocks adhesion of lymphocytes to the endothelial integrin alpha 6 beta 1. *Proc. Natl. Acad. Sci. USA* **90**, 9051-9055.
- Leung, T., Chen, X. Q., Manser, E. and Lim, L.** (1996). The p160 RhoA-binding kinase ROK alpha is a member of a kinase family and is involved in the reorganization of the cytoskeleton. *Mol. Cell. Biol.* **16**, 5313-5327.
- Lynch, E. D., Lee, M. K., Morrow, J. E., Welsh, P. L., Leon, P. E. and King, M. C.** (1997). Nonsyndromic deafness DFNA1 associated with mutation of a human homolog of the *Drosophila* gene *diaphanous*. *Science* **278**, 1315-1318.
- Maas, R. L., Zeller, R., Woychik, R. P., Vogt, T. F. and Leder, P.** (1990). Disruption of formin-encoding transcripts in two mutant *limb deformity* alleles. *Nature* **346**, 853-855.
- Madri, J. A. and Graesser, D.** (2000). Cell migration in the immune system: the evolving inter-related roles of adhesion molecules and proteinases. *Dev. Immunol.* **7**, 103-116.
- Martin, P.** (1997). Wound healing – aiming for perfect skin regeneration. *Science* **276**, 75-81.
- Naviaux, R. K., Costanzi, E., Haas, M. and Verma, I. M.** (1996). The pCL vector system: rapid production of helper-free, high-titer, recombinant retroviruses. *J. Virol.* **70**, 5701-5705.
- Norris, P. S., Jepsen, K. and Haas, M.** (1998). High-titer MSCV-based retrovirus generated in the pCL acute virus packaging system confers sustained gene expression in vivo. *J. Virol. Methods* **75**, 161-167.
- Palecek, S. P., Schmidt, C. E., Lauffenburger, D. A. and Horwitz, A. F.** (1996). Integrin dynamics on the tail region of migrating fibroblasts. *J. Cell Sci.* **109**, 941-952.
- Petersen, J., Weigluny, D., Egel, R. and Nielsen, O.** (1995). Characterization of *fus1* of *Schizosaccharomyces pombe*: a developmentally controlled function needed for conjugation. *Mol. Cell. Biol.* **15**, 3697-3707.
- Pruyne, D., Evangelista, M., Yang, C., Bi, E., Zsigmond, S., Bretscher, A. and Boone, C.** (2002). Role of formins in actin assembly: nucleation and barbed end association. *Science* **297**, 612-615.
- Ridley, A. J. and Hall, A.** (1992). The small GTP-binding protein Rho regulates the assembly of focal adhesions and actin stress fibers in response to growth factors. *Cell* **70**, 389-399.
- Ridley, A. J., Paterson, H. F., Johnson, C. L., Diekmann, D. and Hall, A.** (1992). The small GTP-binding protein Rac regulates growth factor-induced membrane ruffling. *Cell* **70**, 401-410.
- Riveline, D., Zamir, E., Balaban, N. Q., Schwarz, U. S., Ishizaki, T., Narumiya, S., Kam, Z., Geiger, B. and Bershadsky, A. D.** (2001). Focal contacts as mechanosensors: externally applied local mechanical force induces growth of focal contacts by an mDial1-dependent and ROCK-independent mechanism. *J. Cell Biol.* **153**, 1175-1186.
- Sagot, I., Klee, S. K. and Pellman, D.** (2002). Yeast formins regulate cell polarity by controlling the assembly of actin cables. *Nat. Cell Biol.* **4**, 42-50.
- Sotiropoulos, A., Gineitis, D., Copeland, J. and Treisman, R.** (1999). Signal-regulated activation of serum response factor is mediated by changes in actin dynamics. *Cell* **98**, 159-169.
- Tatsis, N., Lannigan, D. A. and Macara, I. G.** (1998). The function of the p190 Rho GTPase-activating protein is controlled by its N-terminal GTP binding domain. *J. Biol. Chem.* **273**, 34631-34638.
- Tominaga, T., Sahai, E., Chardin, P., McCormick, F., Courtneidge, S. A. and Alberts, A. S.** (2000). Diaphanous-related formins bridge Rho GTPase and Src tyrosine kinase signaling. *Mol. Cell* **5**, 13-25.
- Trumpp, A., Blundell, P. A., de la Pompa, J. L. and Zeller, R.** (1992). The chicken *limb deformity* gene encodes nuclear proteins expressed in specific cell types during morphogenesis. *Genes Dev.* **6**, 14-28.
- Umikawa, M., Tanaka, K., Kamei, T., Shimizu, K., Imamura, H., Sasaki, T. and Takai, Y.** (1998). Interaction of Rho1p target Bni1p with F-actin-binding elongation factor 1 alpha: implication in Rho1p-regulated reorganization of the actin cytoskeleton in *Saccharomyces cerevisiae*. *Oncogene* **16**, 2011-2016.
- van der Flier, A. and Sonnenberg, A.** (2001). Function and interactions of integrins. *Cell Tissue Res.* **305**, 285-298.
- Vincent, S. and Settleman, J.** (1999). Inhibition of RhoGAP activity is

- sufficient for the induction of Rho-mediated actin reorganization. *Eur. J. Cell Biol.* **78**, 539-548.
- Vogt, T. F., Jackson-Grusby, L., Rush, J. and Leder, P.** (1993). Formins: phosphoprotein isoforms encoded by the mouse *limb deformity* locus. *Proc. Natl. Acad. Sci. USA* **90**, 5554-5558.
- Wasserman, S.** (1998). FH proteins as cytoskeletal organizers. *Trends Cell Biol.* **8**, 111-115.
- Watanabe, N., Madaule, P., Reid, T., Ishizaki, T., Watanabe, G., Kakizuka, A., Saito, Y., Nakao, K., Jockusch, B. M. and Narumiya, S.** (1997). p140mDia, a mammalian homolog of *Drosophila diaphanous*, is a target protein for Rho small GTPase and is a ligand for profilin. *EMBO J.* **16**, 3044-3056.
- Watanabe, N., Kato, T., Fujita, A., Ishizaki, T. and Narumiya, S.** (1999). Cooperation between mDia1 and ROCK in Rho-induced actin reorganization. *Nat. Cell Biol.* **1**, 136-143.
- Westendorf, J. J.** (2001). The Formin/Diaphanous-related protein, FHOS, interacts with Rac1 and activates transcription from the serum response element. *J. Biol. Chem.* **276**, 46453-46459.
- Westendorf, J. J., Mernaugh, R. and Hiebert, S. W.** (1999). Identification and characterization of a protein containing formin homology (FH1/FH2) domains. *Gene* **232**, 173-182.
- Woychik, R. P., Stewart, T. A., Davis, L. G., D'Eustachio, P. and Leder, P.** (1985). An inherited limb deformity created by insertional mutagenesis in a transgenic mouse. *Nature* **318**, 36-40.
- Woychik, R. P., Maas, R. L., Zeller, R., Vogt, T. F. and Leder, P.** (1990). 'Formins': proteins deduced from the alternative transcripts of the *limb deformity* gene. *Nature* **346**, 850-853.
- Wynshaw-Boris, A., Ryan, G., Deng, C. X., Chan, D. C., Jackson-Grusby, L., Larson, D., Dunmore, J. H. and Leder, P.** (1997). The role of a single formin isoform in the limb and renal phenotypes of limb deformity. *Mol. Med.* **3**, 372-384.
- Yayoshi-Yamamoto, S., Taniuchi, I. and Watanabe, T.** (2000). FRL, a novel formin-related protein, binds to Rac and regulates cell motility and survival of macrophages. *Mol. Cell Biol.* **20**, 6872-6881.
- Yednock, T. A., Cannon, C., Vandevvert, C., Goldbach, E. G., Shaw, G., Ellis, D. K., Liaw, C., Fritz, L. C. and Tanner, L. I.** (1995). Alpha 4 beta 1 integrin-dependent cell adhesion is regulated by a low affinity receptor pool that is conformationally responsive to ligand. *J. Biol. Chem.* **270**, 28740-28750.
- Zahner, J. E., Harkins, H. A. and Pringle, J. R.** (1996). Genetic analysis of the bipolar pattern of bud site selection in the yeast *Saccharomyces cerevisiae*. *Mol. Cell Biol.* **16**, 1857-1870.